



## Evolution of a helper virus-derived, ribosome binding translational enhancer in an untranslated satellite RNA of *Turnip crinkle virus*

Rong Guo<sup>a</sup>, Arturas Meskauskas<sup>a,b</sup>, Jonathan D. Dinman<sup>a</sup>, Anne E. Simon<sup>a,\*</sup>

<sup>a</sup> Department of Cell Biology and Molecular Genetics, University of Maryland College Park, College Park, MD, 20742 USA

<sup>b</sup> Department of Biotechnology and Microbiology, Vilnius University, Lithuania

### ARTICLE INFO

#### Article history:

Received 11 July 2011

Returned to author for revision 27 July 2011

Accepted 31 July 2011

#### Keywords:

Satellite RNA

RNA evolution

RNA conformational shift

RNA structure/function

*Carmovirus*

### ABSTRACT

SatC is a noncoding subviral RNA associated with *Turnip crinkle virus* (TCV). A 100-nt stretch in the 3' UTR of TCV contains three hairpins and two pseudoknots that fold into a tRNA-shaped structure (TSS) that binds 80S ribosomes. The 3' half of satC is derived from TCV and contains 6-nt differences in the TSS-analogous region. SatC binds poorly to 80S ribosomes, and molecular modeling that predicted the 3D structure of the TSS did not predict a similar structure for satC. When the satC TSS region was step-wise converted to the original TCV TSS bases, ribosome binding increased to TCV TSS levels without significantly affecting satC replication. However, mutant satC was less fit when accumulating in plants and gave rise to numerous second site changes that weakened one of two satC conformations. These results suggest that minor changes from the original TCV sequence in satC reflect requirements other than elimination of ribosome binding.

© 2011 Elsevier Inc. All rights reserved.

### Introduction

Regulation of many RNA-associated cellular processes, including termination of transcription, translation, and RNA cleavage, can involve changes in the conformation of the RNA (Brantl, 2004; Nagel and Pleij, 2002). For example, positive sense (+)-stranded RNA viral genomes must initially assume a conformation that is recognized by cellular ribosomes for reiterative translation of products required for replication, such as the viral RNA-dependent RNA polymerase (RdRp). When sufficient RdRp has been synthesized, the RNA must switch to a form that is both inaccessible to ribosomes and contains cis-acting elements necessary to attract the newly translated RdRp (Dreher, 1999; Yuan et al., 2009). Following reiterative transcription of (–)-strand intermediates, (+)-strands are synthesized that may not be templates for further (–)-strand synthesis (Martinez et al., 2011; Zhang and Simon, 2005). This would imply that de novo synthesized (+)-strands may be adopting a conformation that is not recognized by the RdRp. For viral genomic RNAs (gRNAs), this alternative conformation may be the initial translation-competent form.

*Turnip crinkle virus* (TCV; genus *Carmovirus*, family *Tombusviridae*) gRNA encodes five proteins for use in replication, movement and encapsidation (Fig. 1A) (Carrington et al., 1989; Hacker et al., 1992). In addition to its monopartite (+)-sense genome, a field isolate of TCV was found associated with several non-essential satellite (sat)RNAs,

one of which (satC; 356 nt) originated from recombination events between a second satRNA (satD; 194 nt) and two regions from the 3' end of TCV (Simon and Howell, 1986). TCV maintains non-essential satC because the satRNA confers a selective advantage by suppressing virion formation, which enhances RNA silencing suppression conferred by individual capsid proteins, allowing the virus to transit more rapidly through the plant (Zhang and Simon, 2003).

Since TCV satRNAs have no coding capability, their replication and encapsidation are dependent on the RdRp and capsid proteins encoded by TCV. SatRNAs and other untranslated subviral RNAs derived from helper viral genomes must therefore contain cis-sequences and structures recognized by the viral RdRp and thus have become models for identifying and studying helper virus replication elements using smaller, less complex genomes (Chernysheva and White, 2005; Fabian et al., 2003; Simon et al., 2004; Zhang et al., 2004a, 2006b). However, assignment of function for shared elements based solely on roles defined in subviral RNAs can be problematic if minor sequence differences reflect evolution of elements so that they can function independently of viral sequences not present in the subviral RNA. Alternatively, such modifications may disrupt virus-specific elements that inhibit or are not needed for subviral RNA accumulation (e.g., ones required for translation) and/or may allow for the acquisition of new subviral RNA-specific requirements, such as the generation of a pre-active conformation (Zhang et al., 2006a,b).

TCV and its associated satRNAs have no 5' caps or 3' poly(A) tails and terminate their 3' ends with a hydroxyl group. Sequence in the 3' region shared by satC and TCV (90% sequence identity) is predicted by the RNA structure modeling program MPGAfold (Shapiro et al., 2006) to form four hairpins (Fig. 1B) that are all or

\* Corresponding author. Fax: +1 301 805 1318.

E-mail address: [simona@umd.edu](mailto:simona@umd.edu) (A.E. Simon).

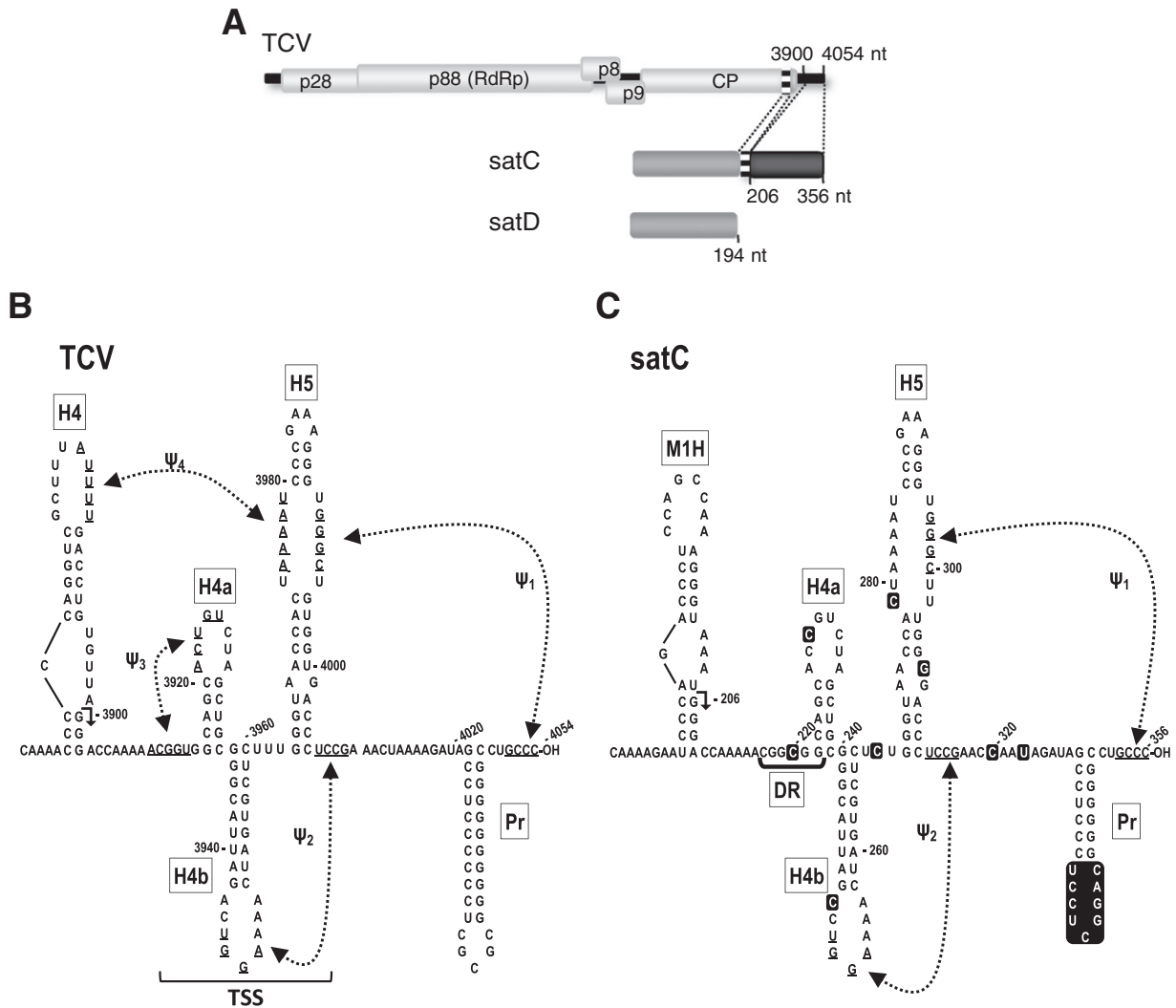


**Fig. 1.** Relationship between TCV and satC. (A) Schematic representation of TCV-associated RNAs. The single (+)-strand genome of TCV and five open reading frames are shown. p28 and the read-through protein p88 (the RdRp) are required for replication. p8 and p9 are required for cell-to-cell virus movement. satC is a chimeric RNA composed of a second satRNA (satD) and two regions from the 3' end of TCV. Numbers and dotted lines indicate satC sequences that are shared with TCV. Similar regions are shaded alike. (B) MPGAfold-predicted TCV and (C) satC 3' structures. Hairpins are described in the text. The region the folds into the T-shaped structure (TSS) in TCV is indicated. Sequence differences between satC and TCV are boxed in the satC sequence. Although the satC structure is shown in a similar configuration as TCV for ease of comparison, none of the hairpins are present in the satC structure assumed by transcripts synthesized *in vitro*, while at least H5 and  $\Psi_1$  are present in the satC replication-active structure (Zhang et al., 2004a,b). H4 and M1H are transcriptional enhancers, and H4 is also a critical element for translation (Sun and Simon, 2006; Yuan et al., 2010). Arrowheads in H4 and M1H denote 5' end of shared 3' terminal sequences.

partially conserved among the *Carmoviruses* (McCormack et al., 2008; Yuan et al., 2010). In satC, these hairpins are thought to be present in the replication-active structure (Zhang et al., 2006a,b), and it is currently not known which hairpins (if any) are also present in the pre-active conformation. Despite sequence conservation in the 3' region of the satRNA and helper virus, satC with the 3' 100 bases of TCV, and TCV with satC 3' 100 bases accumulate very poorly in plants and protoplasts (Wang and Simon, 2000). The residues most responsible for the sequence-specific effects were mapped to the 3' terminal Pr hairpin (Song and Simon, 1995; Sun and Simon, 2006; Zhang et al., 2006c), which in TCV interacts with upstream sequences that are not present in the satRNA (Yuan et al., 2009, 2010). *In vitro* transcription of non-viral fragments directed only by the Pr indicated that the Pr serves as the core promoter, with satC Pr activity significantly higher than that of TCV (Sun and Simon, 2006; Zhang et al., 2006c). These results suggest that the satC Pr has evolved to function in the absence of upstream TCV sequences.

The hairpin upstream of Pr, H5, contains a large symmetrical loop that pairs with 3' terminal bases forming  $\Psi_1$ , which is required for

efficient accumulation of both TCV and satRNA (Fig. 1; McCormack and Simon, 2004; Zhang and Simon, 2005; Zhang et al., 2004b). H4a and H4b function as an interactive unit based on hairpin exchanges with the related *Carmovirus*, *Cardamine chlorotic fleck virus* (McCormack et al., 2008; Zhang et al., 2006b). H4b loop forms a pseudoknot ( $\Psi_2$ ) with sequence just downstream of H5, which is required for both TCV and satC accumulation (McCormack et al., 2008; Zhang et al., 2006b). The loop of H4a forms a pseudoknot with adjacent upstream sequence in TCV and this pseudoknot ( $\Psi_3$ ) is critical for TCV accumulation (McCormack et al., 2008). In contrast,  $\Psi_3$  is not required for satC replication in protoplasts but does appear to contribute to satC fitness in plants (Guo et al., 2009). This difference in  $\Psi_3$  requirements between TCV and satC was attributed to the involvement of  $\Psi_3$ , along with  $\Psi_2$  and hairpins H5, H4a and H4b, in forming a T-shaped structure (TSS) in TCV that functions as part of a 3' cap-independent translational enhancer (3' CITE) (McCormack et al., 2008). The TSS binds to the ribosome P-site through the 60S subunit (Stupina et al., 2008) and is also a stable scaffold for interactions with surrounding sequences, including the Pr (Yuan et al., 2009).

RNA2D3D (Martinez et al., 2008) predicted that the 6-nt differences in satC in the TSS-analogous region produced significant destabilizing effects, with both  $\Psi_2$  and  $\Psi_3$  losing their standard base-pairing interactions (Stupina et al., 2008). In this report, we test the hypothesis that the differences between TCV and satC in the TSS region arose to suppress ribosome binding to satC, which might interfere with satC replication. Stepwise conversion of satC residues to their TCV counterparts in the satC TSS-analogous region substantially enhanced ribosome binding to the satRNA, particularly a single base transversion in the loop of H4b. Enhanced ribosome binding, however, had no discernable correlative structural changes in the satRNA and no negative effect on satRNA replication in protoplasts. All changes, however, impacted fitness of satC in plants. This suggests that satC evolved to eliminate the TSS for reasons other than reducing ribosome binding.

## Results and discussion

### Ribosome binding is enhanced in satC mutants containing TCV residues in the TSS-analogous region

The 3' proximal placement of translational enhancers near elements required for (–)-strand synthesis in small plant RNA viruses suggests that regional conformational changes might control the switch between the incompatible activities of translation and replication (Yuan et al., 2009). Since untranslated subviral RNAs no longer require maintenance of any translation elements, specific alterations in 3' helper virus-derived sequence might have arisen to strengthen replication elements without a need to maintain the

original role in translation. The unusual feature of a ribosome-binding internal tRNA-like structure in the 3' region of TCV allowed us to question whether specific changes in satC were primarily intended to eliminate the TSS and its presumptive interference on replication when bound to ribosomes, or whether the changes simply allowed for more efficient replication of the satRNA or enhancement of some other attribute.

SatC contains 6-nt differences with TCV in the TSS-analogous region (Fig. 1C): C229U and C220U in  $\Psi_3$ -H4a, C249A in H4b loop, C268U between H4b and H5, and two changes in H5 (using our nomenclature, the satC-specific base precedes its location in the satC genome followed by the TCV-specific base). The two alterations in H5 were thought less likely to contribute substantially to ribosome binding since ribosome binding occurs in the absence of H5 (Stupina et al., 2008) and replication of satC was not negatively affected when containing TCV H5 (Zhang et al., 2006c). The remaining four changes are distributed throughout the upper portion of the TSS (Figs. 2A and B).

The TSS-analogous region in satC (positions 216–315) was an inefficient ribosome-binding template (Stupina et al., 2008), while full length satC bound ribosomes detectably, with a  $K_d$  of  $12.14 \times 10^{-6}$  M, about 27-fold weaker than ribosome binding to the TCV TSS (Fig. 2C). Since full-length satC gave measurable levels of ribosome binding, all binding assays for this report were conducted using full-length satC. To determine which of these 4-nt differences between TCV and satC were responsible for reduced ribosome binding and whether gain of ribosome binding would impact satC replication, we first converted all four alterations in the TSS-analogous region of satC to their TCV counterparts (Fig. 2A). SatC with the four TCV residues (C220U/C229U/C249A/C268U)

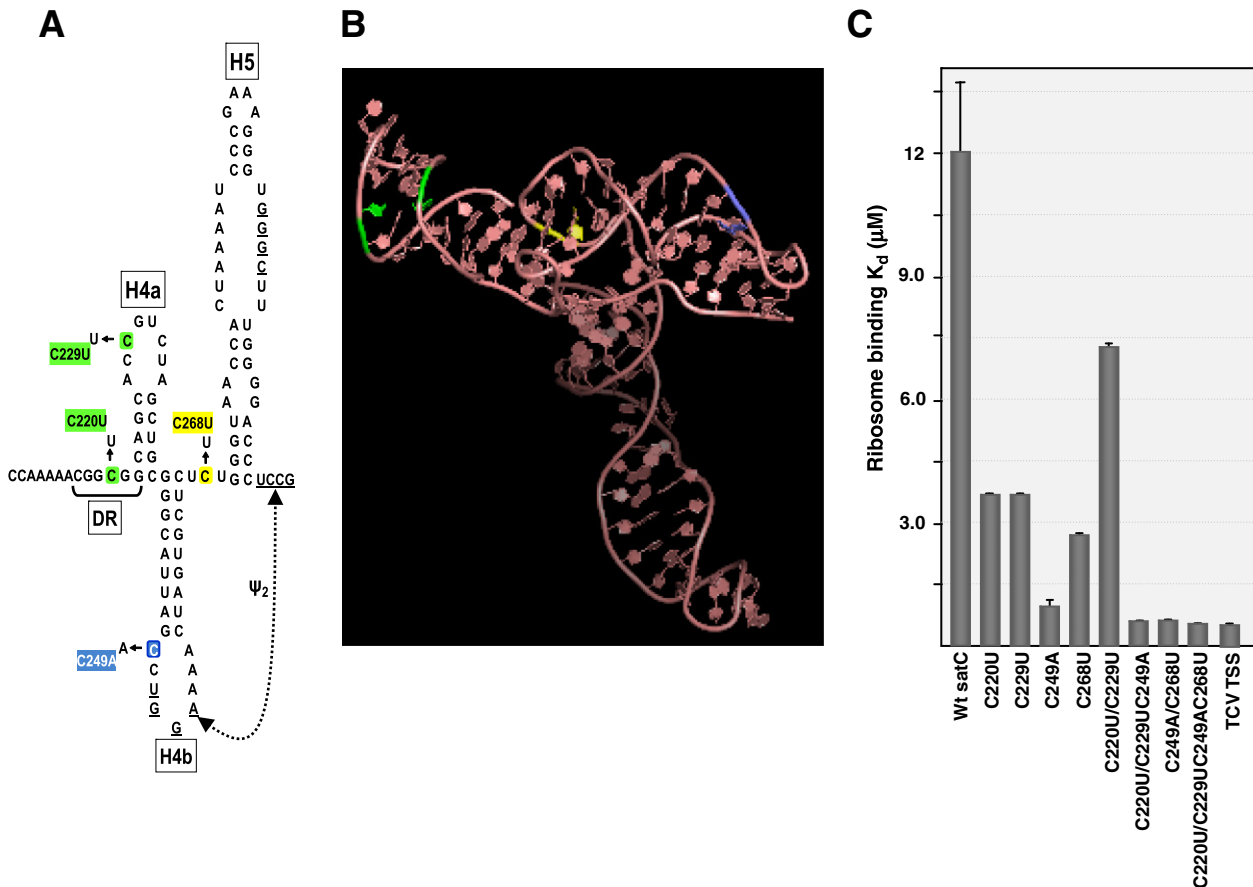


**Fig. 2.** Ribosome binding of satC mutants containing TCV TSS sequence. (A) SatC TSS analogous region. Location of nucleotide differences is indicated. Colors of particular alterations correspond with their location in the TSS structure. (B) 3D structure of the TCV TSS determined by NMR and SAXS [small angle x-ray scattering; (Zuo et al., 2010)]. Locations of nucleotide differences with satC are color coded as in (A). (C) 80S ribosome binding of satC mutants. Filter binding assays were performed in triplicate and standard error is given.

bound ribosomes at near TCV TSS levels ( $K_d = 0.55 \times 10^{-6}$  M, compared with TCV TSS  $K_d = 0.45 \times 10^{-6}$  M; Fig. 2C). This result indicates that the two altered positions within H5 that remained as satC-specific residues are not contributing substantially to ribosome binding.

To determine which of the four positions, or combination of positions, were principally responsible for recovery of ribosome binding, the four satC-specific residues were converted independently to their TCV counterparts (Fig. 2A). The most substantial increase in ribosome binding due to alteration of an individual position was the 12-fold enhancement achieved when satC contained the TCV-specific residue at position 249 in the loop of H4b (C249A;  $K_d = 0.99 \times 10^{-6}$  M). SatC with the TCV residue in the short linker between H4b and H5 (C268U) also improved ribosome binding, with the  $K_d$  decreased 4.4-fold to  $2.75 \times 10^{-6}$  M.

Altering the individual residues in  $\Psi_3$ /H4a (C220U or C229U) also enhanced ribosome binding by similar 3.2-fold levels (Fig. 2C). Combining the latter two alterations to generate TCV-equivalent H4a and  $\Psi_3$  unexpectedly reduced ribosome affinity by 1.9-fold compared with the individual changes (Fig. 2C). In contrast, combining C220U/C229U with C249A improved ribosome binding to near wt TCV TSS levels, as did the combination of C268U and C249A. These results indicate that while conversion of all four satC-specific residues enhanced ribosome binding to satC, C249A located in the loop of H4b but outside of  $\Psi_2$  had the most significant effect in improving satC binding to 80S ribosomes,

#### *SatC with TCV TSS sequence causes structural changes in $\Psi_2$ and H4a*

Full length wt satC and satC mutants with combinations of TCV-specific residues in the TSS-equivalent region were subjected to in-line probing to determine if enhanced ribosome binding correlated with any discernable structural differences. In-line structure probing monitors the amount of phosphodiester bond cleavage in the RNA backbone (Soukup and Breaker, 1999). Cleavage is caused by a nucleophilic attack of the 2' oxygen on the proximal backbone phosphate when the 2' oxygen, phosphate and oxyanion leaving group adopt a linear configuration. Since this configuration occurs if the residue is flexible and able to rotate, i.e., not overly constrained by higher-order structure, in-line probing can monitor the flexibility of each residue in an RNA fragment with the degree of cleavage proportional to its relative flexibility. We chose to examine three of the satC mutants: C249A and C268U, since both significantly enhanced ribosome binding; and C220U/C229U/C249A/C268U, which had the highest affinity for ribosomes.

In-line probing of wt and all mutant satC produced no discernable differences in the cleavage pattern in the 5' half of the satC genomes (data not shown). In the satRNA 3' half, wt satC and C268U had similar cleavage patterns (Fig. 3C) despite 4.4-fold differences in ribosome-binding properties, suggesting that ribosome binding is not associated with any major changes discernable by in-line probing. C268 and adjacent nucleotides in the linker between H5 and H4b are highly flexible in satC [as is the equivalent region in TCV (McCormack et al., 2008)] and transition to the TCV uridylylate at this position had no effect on the local structure. This suggests that a uridylylate in this position, and not the local structure, is important for ribosome binding.

C249A enhanced the flexibility of two nearby residues in the loop of H4b (U251 and A254). This enhanced flexibility was retained in C220U/C229U/C249A/C268U. These H4b loop residues participate in  $\Psi_2$ , suggesting that C249A may be weakening  $\Psi_2$ . C220U/C229U/C249A/C268U also produced additional cleavage pattern alterations in the loop of H4a due to inclusion of C220U and C229U in this construct. However, none of these minor structural alterations were present in all mutants. These results suggest that individual residues are affecting ribosome interaction in the region, and acquisition of ribosome binding capability is not associated with any major structural changes that are discernable by in-line probing.

#### *Effect of enhanced ribosome binding on satRNA accumulation in protoplasts and plants*

To determine if the enhanced ability of satC mutants to bind ribosomes interferes with replication, satC containing the single and multiple base changes described in Fig. 2 were inoculated onto protoplasts with TCV helper virus and satRNA levels assayed at 40-hours postinoculation. As part of a separate study, we previously found that C268U reproducibly accumulated to greater than wt levels in protoplasts (110%; Zhang et al., 2006c). Accumulation of satC with the other single/combinations of TCV-specific residues ranged from 98% to 123% of wt, indicating either that ribosome binding does not interfere with satC replication or that the satRNA is not exposed to ribosomes in the cell (Fig. 4B). Interestingly, satC containing the two TCV residues in H5 (U302G/G306U) or C279A, all of which strengthen the stem of H5 and thus the satC active structure, also accumulated to levels 10 to 15% higher than wt in protoplasts as did several of the mutants in this study (Fig. 4; Zhang et al., 2006a,c). It is possible, therefore, that alterations producing low but reproducible enhancement of satC accumulation are similarly stabilizing the active form of satC.

Accumulation of satC in protoplasts is a function of replication competence and the stability of the RNA. Accumulation of satRNAs in plants includes these functions as well as the ability to move cell-to-cell and long distances, which may include encapsidation efficiency. In addition, the capability of a satRNA to suppress the silencing machinery of the host can affect the level of helper virus, which impacts satRNAs dependent on products encoded by the helper virus. To determine if the TCV TSS residues reduce the ability of mutant satC to compete with wt satC, equal amounts of C249A, C268U, and C220U/C229U/C249A/C268U transcripts were combined with wt satC transcripts and inoculated onto six turnip seedlings along with TCV gRNA transcripts. At 3-weeks postinoculation, total RNA was extracted from uninoculated upper leaves, followed by full-length satC amplification and cloning from the pooled RNA.

Sequencing of 69 cloned progeny revealed that 45% were wt satC (Table 1). This result indicates that mutant satC were less fit than wt, despite the equal or greater capacity to replicate in protoplasts. Of the three original input mutant sequences recovered, C249A comprised the majority of recovered clones (27%). Additionally, 13 of the 69 full-length cloned satC contained altered residues not present in the inoculated transcripts. Six of these second-site changes were found alone in an otherwise wt background and the remaining 7 contained various combinations of parental mutations and second-site changes. Since we previously sequenced 25 full-length progeny of wt satC and found no sequence differences (Zhang et al., 2004b), it is likely that satC with second site changes, but no primary site alterations, represent progeny of mutant satC whose initial mutations reverted following acquisition of the second-site change. Consistent with this interpretation, two of the progeny of C220U/C229U/C249A/C268U had reverted C268U to the satC-specific residue, and one of these also contained second-site mutations. No clones were recovered with only C268U or C268U and second-site changes, suggesting that this TCV-specific residue is poorly compatible with satC background sequence. Interestingly, the untranslated TCV DI-RNA diG also contains the satC-specific cytidylate in this location (Li et al., 1989). diG has only one other base variation with TCV in the TSS region, a cytidylate that enlarges the H5 lower symmetrical loop.

Second-site alterations were present throughout satC, from position 51 to position 273. Six of the second-site changes were in the satD-derived 5' region and 8 were in the 3' TCV-related half (Fig. 5). Of these 8 changes, six were predicted to weaken the four hairpin, two pseudoknot active structure of satC. These were: i. U312C eliminated a canonical A:U base-pair in  $\Psi_2$ ; ii. U273C eliminated a U:A pair in the lower stem of H5; iii. CUC266AGG substantially weakened the lower stem of H4b by eliminating three base-pairs; and iv. C239U

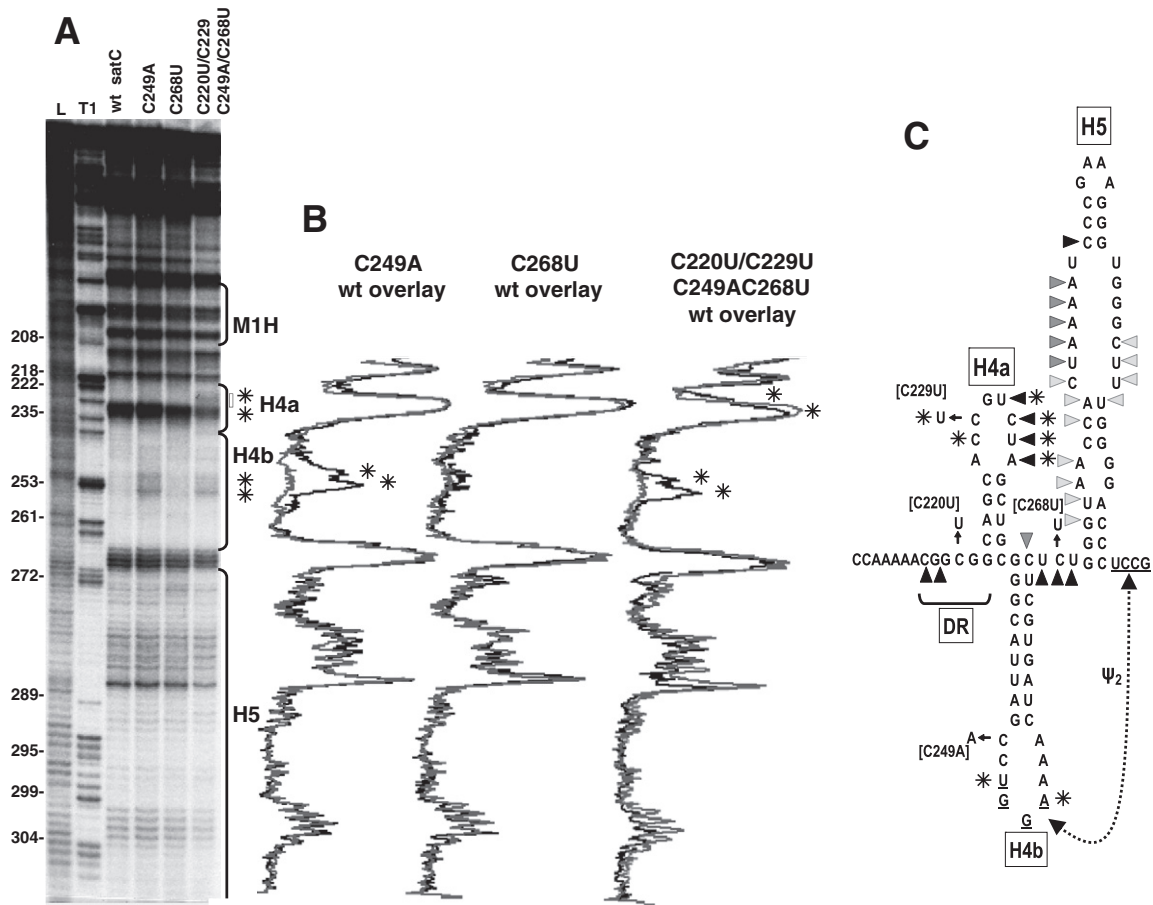


**Fig. 3.** In-line probing of the 3' half of wt satC and various mutants. (A) Autoradiograph of a typical in-line probing of satC wt and mutant RNAs. Numbering is from the 5' end of satC. L, partial hydroxide cleavage ladder; T1, partial RNase T1 digestion of denatured RNA showing the location of guanylates. Locations of the hairpins are indicated to the right. Asterisks indicate differences between wt satC and C249A or C220U/C229U/C249A/C268U. (B) Overlays of densitometer tracings from mutant (dark tracings) and wt satC (light tracings). Asterisks denote consistent differences between mutant and wt satC from three in-line probeings. (C) Position of residues susceptible to in-line cleavage. Darker triangles denote more intense cleavages. Asterisks denote location of nucleotides with enhanced susceptibility in C249A and C220U/C229U/C249A/C268U relative to wt satC.

changed a G:C pair at the base of H4a to a G:U pair. Of the remaining two second-site changes, one was in the loop of M1H and one was in the DR region. While mutations in the DR region are known to affect the satC conformational switch, it is not known if this particular mutation also affects the active structure of satC (Zhang et al., 2006a, b).

Although the structural changes caused by incorporation of TCV-specific residues into the satC TSS-analogous region remain unknown, it is logical to assume that they produce a more TCV-like 3D structure, since the changes correlate with improved ribosome binding. Our current model is that the TCV-like structure is the active structure of satC and thus these alterations had either no negative effect or a small positive effect on satC accumulation in single cells. Since there are no discernable connections between specific primary mutations and the associated second-site changes, our results suggest that the second site changes represent an attempt to weaken the active satC structure as opposed to compensating for specific initial mutations. In conclusion, while the satRNA-specific residues in the TSS-analogous region decrease satC affinity for ribosomes, these alterations were not needed for satC replication. We hypothesize instead that the satC-specific residues evolved to subtly weaken the satC active structure to support a “pre-active” (replication-resistant) structure assumed by newly synthesized (+)-strands. The formation of a pre-active structure would suppress transcription errors associated with geometric replication and instead lead to (+)-strand “stamping” off of (–)-strands that are generated from the originally infecting (+)-strand templates (Martinez et al., 2011), thus enhancing the fitness of the satRNA.

## Materials and methods

### Construction of satC mutants

To generate plasmid C220U, C229U, C220U/C229U, and C249A, PCR reactions were performed using template pT7C+, which contains full-length satC downstream from a T7 polymerase promoter. Primers were a common 5' primer containing the T7 RNA polymerase promoter and 19 nt from the 5' end of satC (T7C5', GTAATACGACTACTATAGGATAACTAAGGGTTTCA) and 3' primers containing the SpeI site and site-specific mutations. SpeI- and NcoI-digested PCR products were ligated into similarly digested pT7C+, replacing the endogenous fragment. To construct plasmid C220U/C229U/C249A, PCR products generated using template C220U/C229U were digested with SpeI and NcoI, and the fragments inserted into similarly treated pT7C+. To construct plasmid C249A/C268U and C220U/C229U/C249A/C268U, PCR reactions were performed using template C268U or C220U/C229U. SpeI- and NcoI-digested PCR products were inserted into the analogous region of plasmid C268U or C220U/C229U. All constructs were confirmed by DNA sequencing.

### Isolation of 80S ribosomes

Yeast ribosomes (strain JD1090) were isolated as previously described (Meskauskas et al., 2005). Supernates following cellular disruption were transferred to 4 ml polycarbonate tubes containing

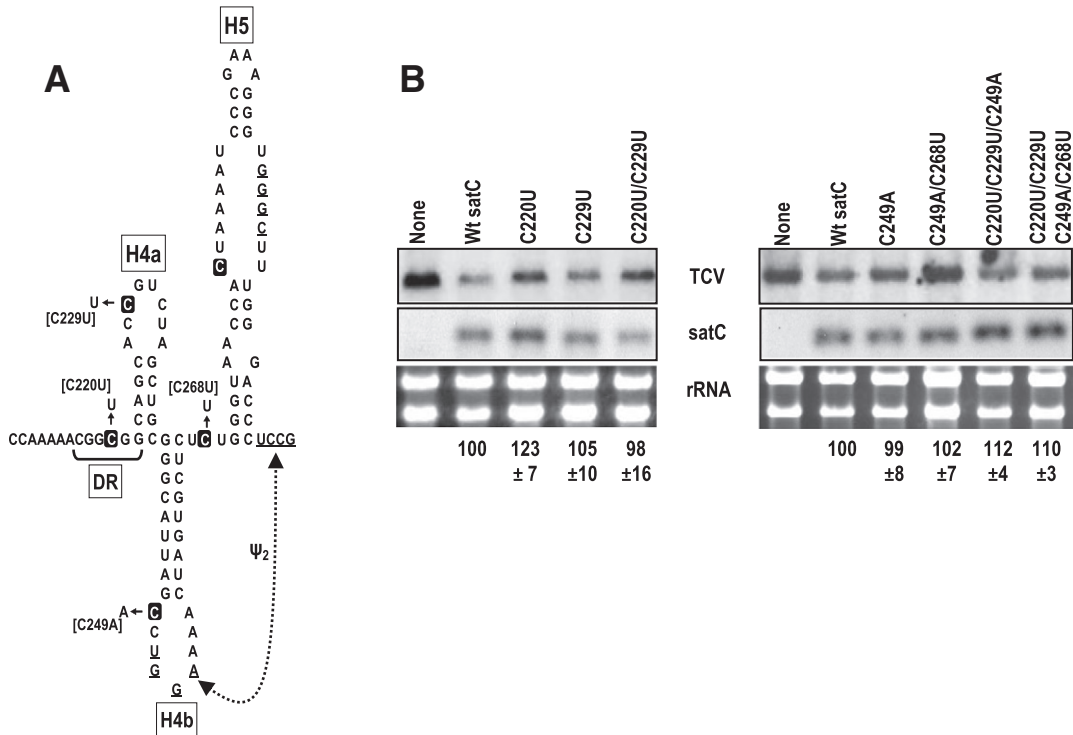


**Fig. 4.** Replication of satC mutants with TCV TSS nucleotides. (A) SatC TSS analogous region with the location of the 4 nt differences with TCV. (B) Accumulation at 40 h postinoculation of satC wt and mutants in *Arabidopsis* protoplasts co-inoculated with helper TCV gRNA. Total extracted RNA was hybridized with a [ $\gamma$ - $^{32}$ P]ATP-labeled oligonucleotide probe complementary to both satC and TCV. Data from three independent experiments were adjusted for rRNA levels and then normalized to wt satC levels, arbitrarily assigned a value of 100. Standard deviation is given.

1 ml of cushion buffer C [50 mM Tris-HCl, pH 7.5 at 4 °C, 5 mM Mg (CH<sub>3</sub>COO)<sub>2</sub>, 50 mM NH<sub>4</sub>Cl, 25% glycerol, 0.1 mM PMSF, 0.1 mM DTE]. Ribosomes were sedimented by centrifugation for 2 h at 50,000 rpm using an MSL-50 rotor. Fines from ribosome pellets were gently washed off with buffer C. Ribosomes were suspended in buffer C at concentrations of 2 to 10 pmol/μl (1 OD<sub>260</sub> = 20 pmol) and stored frozen at -80 °C.

*Ribosome binding assays*

Filter binding assays were performed as previously described (Meskauskas et al., 2005) in 50 μl of binding buffer [80 mM Tris-HCl pH

7.4, 160 mM NH<sub>4</sub>Cl, 11 mM Mg(CH<sub>3</sub>COO)<sub>2</sub>, 6 mM β-mercaptoethanol, 0.4 mM GTP, and 2 mM spermidine, 0.4 μg/ml of poly(U)] containing 25 pmol of ribosomes and 2–100 pmol of [ $\gamma$ - $^{32}$ P]ATP 5'-end labeled RNA.

**Table 1**

Competition between wt and mutant satC in plants.

Mutations	Recovered sequences	Number recovered
Competition (wt, C249A, C268U, C220U/C229U, C220U/C229U/C249A/C268U)	wt C249A C268U C220U/C229U C220U/C229U/C249A/C268U	31 19 0 2 1
	<b>G142A</b> <b>G157A</b> <b>C190U</b> <b>A216G</b> C220U <b>U312C</b> <b>A51G/C220U/C229U</b> C220U/C229U/C249A <b>U159C/C220U/C229U/C249A/C268U</b> <b>U159C/C220U/C229U/C249A/U273C</b> <b>U115 insertion/C239U/C249A</b> C249A/ <b>C264G/U265G/C266A</b>	1 2 1 2 1 1 1 1 1 1 1 3 1

Second site changes are in bold.

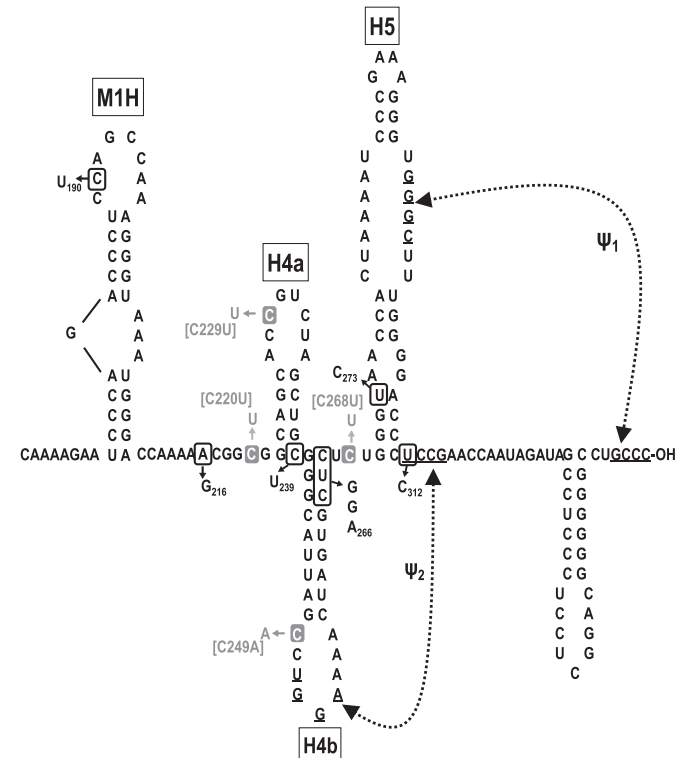


**Fig. 5.** Location of second-site mutations in the 3' region of satC. See Table 1 for a list of all second-site alterations. Position of primary mutations is in gray.

### *In vitro* transcription, inoculation of *Arabidopsis* protoplasts, and Northern blots

TCV genomic and satC RNA transcripts with precise 5' and 3' ends were synthesized using T7 RNA polymerase and SmaI-digested plasmids. Protoplasts ( $5 \times 10^6$ ), prepared from callus cultures of *Arabidopsis thaliana* ecotype Col-0, were inoculated with 20  $\mu\text{g}$  of genomic RNA transcripts with and without 2  $\mu\text{g}$  of satC transcripts using PEG–CaCl<sub>2</sub>, as previously described (Kong et al., 1997). Total RNA was isolated from protoplasts at 40 hpi, denatured using formamide and separated on non-denaturing agarose gels as previously described (Wang and Simon, 1999). Subsequently denatured RNA was hybridized with a [ $\gamma$ -<sup>32</sup>P]ATP-labeled oligonucleotide probe oligo 13 (GTTACCCAAAGAGCACTAGTT), which is complementary to both satC and TCV sequence.

### RNA in-line probing

In-line probing was performed essentially as previously described (Yuan et al., 2009). Briefly, full length wt satC and mutants C249A, C268U, C220U/C229U/C249A/C268U were synthesized using T7 RNA polymerase, and then purified by agarose gel electrophoresis. RNAs were ligated with [ $\alpha$ -<sup>32</sup>P]pCp by T4 RNA ligase, and then purified with 5% polyacrylamide gel. Radiolabeled RNAs were heated to 95 °C for 5 min and snap cooled on ice for 3 min. RNA (20 pmol) was then incubated at room temperature in 50 mM Tris–HCl (pH 8.5), 20 mM MgCl<sub>2</sub>, 100 mM NaCl for 14 h. Reactions were then inactivated and ethanol precipitated. Samples with RNA loading buffer (Ambion) added were heat denatured at 95 °C for 2 min, and subjected to electrophoresis through sequencing length 8% denaturing polyacrylamide gels containing 8 M urea.

### Competition in plants

5  $\mu\text{g}$  of T7 generated in vitro transcripts of wt satC, mutants C249A, C268U, C220U/C229U, C220U/C229U/C249A/C268U and 2  $\mu\text{g}$  of wt TCV transcripts were co-inoculated onto 6 turnip seedlings. Total RNA was extracted from un-inoculated leaves at 21 days post inoculation (dpi). Full-length satC amplified by reverse transcription-PCR (RT-PCR) with primers T7C5' and oligo 7 were cloned into the SmaI site of pUC19 and then sequenced.

### Acknowledgments

This work was supported by a grant from the U.S. Public Health Service (GM 061515-05A2/G120CD1) to A.E.S., the U.S. Public Health Service (GM R01058859) to J.D. and the American Heart Association to A.M. (AHA 0630163N). RG was supported by NIH Institutional Training Grant 2T32AI051967-06A1.

### References

Brantl, S., 2004. Bacterial gene regulation: from transcription attenuation to riboswitches and ribozymes. *Trends Microbiol.* 12, 473–475.  
 Carrington, J.C., Heaton, L.A., Zuidema, D., Hillman, B.L., Morris, T.J., 1989. The genome structure of *Turnip crinkle virus*. *Virology* 170, 219–226.  
 Chernysheva, O.A., White, K.A., 2005. Modular arrangement of viral cis-acting RNA domains in a tomosvirus satellite RNA. *Virology* 332, 640–649.  
 Dreher, T.W., 1999. Functions of the 3'-untranslated regions of positive strand RNA viral genomes. *Ann. Rev. Phytopathol.* 37, 151–174.  
 Fabian, M.R., Na, H., Ray, D., White, K.A., 2003. 3'-terminal RNA secondary structures are important for accumulation of tomato bushy stunt virus DI RNAs. *Virology* 313, 567–580.

Guo, R., Lin, W., Zhang, J.C., Simon, A.E., Kushner, D.B., 2009. Structural plasticity and rapid evolution in a viral RNA revealed by in vivo genetic selection. *J. Virol.* 83, 927–939.  
 Hacker, D.L., Petty, I.T.D., Wei, N., Morris, T.J., 1992. *Turnip crinkle virus* genes required for RNA replication and virus movement. *Virology* 186, 1–8.  
 Kong, Q.Z., Wang, J.L., Simon, A.E., 1997. Satellite RNA-mediated resistance to *Turnip crinkle virus* in *Arabidopsis* involves a reduction in virus movement. *Plant Cell.* 9, 2051–2063.  
 Li, X.H., Heaton, L.A., Morris, T.J., Simon, A.E., 1989. *Turnip crinkle virus* defective interfering RNAs intensify viral symptoms and are generated de novo. *Proc. Natl. Acad. Sci. U. S. A.* 86, 9173–9177.  
 Martinez, H.M., Maizel, J.V., Shapiro, B.A., 2008. RNA2D3D: a program for generating, viewing, and comparing 3-dimensional models of RNA. *J. Biomol. Struct. Dyn.* 25, 669–683.  
 Martinez, F., Sardanyes, J., Elena, S.F., Daros, J.-A., 2011. Dynamics of a plant RNA virus intracellular accumulation: stamping machine vs. geometric replication. *Genetics* 188, 637–646.  
 McCormack, J.C., Simon, A.E., 2004. Biased hypermutagenesis associated with mutations in an untranslated hairpin of an RNA virus. *J. Virol.* 78, 7813–7817.  
 McCormack, J.C., Yuan, X.F., Yingling, Y.G., Kasprzak, W., Zamora, R.E., Shapiro, B.A., Simon, A.E., 2008. Structural domains within the 3' untranslated region of *Turnip crinkle virus*. *J. Virol.* 82, 8706–8720.  
 Meskauskas, A., Petrov, A.N., Dinman, J.D., 2005. Identification of functionally important amino acids of ribosomal protein L3 by saturation mutagenesis. *Mol. Cell. Biol.* 25, 10863–10874.  
 Nagel, J.H.A., Pleij, C.W.A., 2002. Self-induced structural switches in RNA. *Biochimie* 84, 913–923.  
 Shapiro, B.A., Kasprzak, W., Grunewald, C., Aman, J., 2006. Graphical exploratory data analysis of RNA secondary structure dynamics predicted by the massively parallel genetic algorithm. *J. Mol. Graph. Model.* 25, 514–531.  
 Simon, A.E., Howell, S.H., 1986. The virulent satellite RNA of *Turnip crinkle virus* has a major domain homologous to the 3' end of the helper virus genome. *EMBO J.* 5, 3423–3428.  
 Simon, A.E., Roossinck, M.J., Havelda, Z., 2004. Plant virus satellite and defective interfering RNAs: new paradigms for a new century. *Ann. Rev. Phytopathol.* 42, 415–437.  
 Song, C.Z., Simon, A.E., 1995. Synthesis of novel products in vitro by an RNA-dependent RNA-polymerase. *J. Virol.* 69, 4020–4028.  
 Soukup, G.A., Breaker, R.R., 1999. Relationship between internucleotide linkage geometry and the stability of RNA. *RNA* 5, 1308–1325.  
 Stupina, V.A., Meskauskas, A., McCormack, J.C., Yingling, Y.G., Shapiro, B.A., Dinman, J.D., Simon, A.E., 2008. The 3' proximal translational enhancer of *Turnip crinkle virus* binds to 60S ribosomal subunits. *RNA* 14, 2379–2393.  
 Sun, X.P., Simon, A.E., 2006. A cis-replication element functions in both orientations to enhance replication of *Turnip crinkle virus*. *Virology* 352, 39–51.  
 Wang, J.L., Simon, A.E., 1999. Symptom attenuation by a satellite RNA in vivo is dependent on reduced levels of virus coat protein. *Virology* 259, 234–245.  
 Wang, J.L., Simon, A.E., 2000. 3'-end stem-loops of the subviral RNAs associated with *Turnip crinkle virus* are involved in symptom modulation and coat protein binding. *J. Virol.* 74, 6528–6537.  
 Yuan, X.F., Shi, K.R., Meskauskas, A., Simon, A.E., 2009. The 3' end of *Turnip crinkle virus* contains a highly interactive structure including a translational enhancer that is disrupted by binding to the RNA-dependent RNA polymerase. *RNA* 15, 1849–1864.  
 Yuan, X.F., Shi, K.R., Young, M.Y.L., Simon, A.E., 2010. The terminal loop of a 3' proximal hairpin plays a critical role in replication and the structure of the 3' region of *Turnip crinkle virus*. *Virology* 402, 271–280.  
 Zhang, F.L., Simon, A.E., 2003. Enhanced viral pathogenesis associated with a virulent mutant virus or a virulent satellite RNA correlates with reduced virion accumulation and abundance of free coat protein. *Virology* 312, 8–13.  
 Zhang, J.C., Simon, A.E., 2005. Importance of sequence and structural elements within a viral replication repressor. *Virology* 333, 301–315.  
 Zhang, G.H., Zhang, J.C., Simon, A.E., 2004a. Repression and derepression of minus-strand synthesis in a plus-strand RNA virus replicon. *J. Virol.* 78, 7619–7633.  
 Zhang, J.C., Stuntz, R.M., Simon, A.E., 2004b. Analysis of a viral replication repressor: sequence requirements for a large symmetrical internal loop. *Virology* 326, 90–102.  
 Zhang, G.H., Zhang, J.C., George, A.T., Baumstark, T., Simon, A.E., 2006a. Conformational changes involved in initiation of minus-strand synthesis of a virus-associated RNA. *RNA* 12, 147–162.  
 Zhang, J.C., Zhang, G.H., Guo, R., Shapiro, B.A., Simon, A.E., 2006b. A pseudoknot in a preactive form of a viral RNA is part of a structural switch activating minus-strand synthesis. *J. Virol.* 80, 9181–9191.  
 Zhang, J.C., Zhang, G.H., McCormack, J.C., Simon, A.E., 2006c. Evolution of virus-derived sequences for high-level replication of a subviral RNA. *Virology* 351, 476–488.  
 Zuo, X.B., Wang, J.B., Yu, P., Eyller, D., Xu, H., Starich, M.R., Tiede, D.M., Simon, A.E., Kasprzak, W., Schwieters, C.D., Shapiro, B.A., Wang, Y.X., 2010. Solution structure of the cap-independent translational enhancer and ribosome-binding element in the 3' UTR of *Turnip crinkle virus*. *Proc. Natl. Acad. Sci. U. S. A.* 107, 1385–1390.